

Li tunneling effects on spin-lattice relaxation rates of a color center in CaO:Li

D. G. Stinson* and H. J. Stapleton

Department of Physics and Materials Research Laboratory, University of Illinois at Urbana—Champaign, Urbana, Illinois 61801

(Received 20 December 1982)

Low-temperature spin-lattice relaxation rates of the $[F_{Li}]^0$ center in single crystals of CaO:Li at X - and Ku -band microwave frequencies exhibit an anisotropy in the functional form of the temperature dependence: from T in the $[100]$ direction to $\text{csch}(25/T)$ in the $[111]$ direction. A model involving longitudinal and transverse tunneling of a Li ion adjacent to the trapped electron can qualitatively explain this and most of the other characteristics of the relaxation data, with the exception of the hyperfine dependence.

I. INTRODUCTION

Imperfect crystals and amorphous materials have additional modes of excitation which are not found in perfect crystals. These new modes modify the optical, thermal, and electric properties of the material. One such mode is the quantum tunneling of low-mass atomic and molecular impurities in crystals.^{1,2} These localized tunneling states (LTS) have been invoked to explain the anomalous low-temperature thermal and dielectric properties of amorphous materials.^{3,4}

These excitations also provide a mechanism for the thermalization of electron spins. The first observation of electron spin-lattice relaxation (SLR) attributed to tunneling was made by Feldman, Castle, and Wagner⁵ from atomic hydrogen in fused silica. Murphy⁶ used rate equation arguments to show that the SLR rate $1/T_1$ would be proportional to $\text{csch}(E/kT)$, where E is the energy splitting due to tunneling, k is Boltzmann's constant, and T is the temperature. Similar behavior has also been observed from the $F_4(\text{Li})$ center in single crystals of lithium-doped KBr.⁷⁻¹²

Kurtz and Stapleton^{13,14} observed an anomalous SLR rate for an F^+ center in the prototype glasses Na, Li, and K β -alumina. They presented a theory based on tunneling states which predicted the magnetic field and temperature dependence of the SLR rate. The isotropic hyperfine (hf) interaction $a\vec{I}\cdot\vec{S}$ provided the coupling between the electron spin \vec{S} of the F^+ center and a tunneling nucleus of spin \vec{I} . In a glass there is a broad distribution of tunneling-state energies. The results for the F^+ center were explained by assuming relaxation through tunneling states whose energies follow a distribution function very close to that determined from measurements of the specific heat,¹⁵ thermal conductivity,¹⁶ and dielectric susceptibility^{17,18} of those materials.

Those results indicated that electron spin-lattice relaxation can be a valuable probe of amorphous materials, particularly if the electron spin-tunneling-state interaction is well understood. In this paper we present an experimental and theoretical investigation of this interaction. As a model system we study the spin-lattice relaxation of a paramagnetic defect adjacent to a tunneling ion: the $[F_{Li}]^0$ center in Li-doped calcium oxide.

In single crystals such as CaO:Li the tunneling states should have well-defined energies. This eliminates having to average over some distribution function which is not known *a priori*, as is necessary in amorphous materials. In addition, the $[F_{Li}]^0$ center, unlike the F center in the alkali halides, has a well-resolved hyperfine structure. This allows measurement of the SLR rate as a function of the nuclear magnetic quantum number m .

Measurements of the SLR rate as a function of temperature, applied magnetic field, crystal orientation, and quantum number m are presented. These results are not consistent with conventional phonon-driven relaxation of F -type centers. In particular we report the first observation of an anisotropic temperature dependence of the SLR data. The theory presented by Kurtz and Stapleton is expanded to cover these new measurements. We show that both the isotropic and anisotropic components of the hf interaction are required to understand the spin-tunneling-state interaction.

II. EXPERIMENTAL RESULTS

The undoped and Li-doped CaO single crystals used in this study were grown by the arc-fusion technique¹⁹ from CaCO_3 and a mixture of CaCO_3 and 5 mol % Li_2CO_3 , respectively. The final concentration of Li in the doped sample was 0.004 wt.% (1.6×10^{-2} % of all atoms). A small amount of

carbon was added to enhance the production of oxygen vacancies. As grown, the doped crystals contain a paramagnetic color center whose X-band electron paramagnetic resonance (EPR) spectrum is shown in Fig. 1 for the case of the applied magnetic field $\vec{H}_0 \parallel [100]$. The spectrum consists of four equally spaced lines, with one set twice as intense as the other. There is also a strong isotropic central peak due to F^+ centers without nearby Li^+ ions.

This spectrum has been identified by Abraham *et al.*²⁰ as due to an electron trapped at a oxygen vacancy adjacent to a substitutional Li impurity. The structure of this center, designated $[F_{\text{Li}}]^0$, is shown in Fig. 2. An anisotropic hf interaction between the electron spin and the Li nuclear spin ($I = \frac{3}{2}$) produces the four hf lines for each of the three axis orientations of the $[F_{\text{Li}}]^0$ centers. This spectrum can be described by the spin Hamiltonian²⁰

$$\mathcal{H} = \mu_B \vec{S} \cdot \vec{g} \cdot \vec{H}_0 + \vec{S} \cdot \vec{A} \cdot \vec{I} . \quad (1)$$

The tensors \vec{g} and \vec{A} display axial symmetry with $g_{\parallel} = 1.9993(3)$, $g_{\perp} = 2.0001(2)$, $a = (A_{\parallel} + 2A_{\perp})/3 = 6.583(5)$ MHz, and $b = (A_{\parallel} - A_{\perp})/3 = 1.213(5)$ MHz. Undoped crystals contain F^+ centers with $g = 2.0001(2)$.

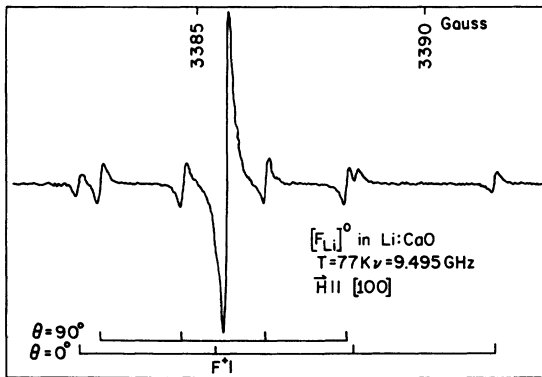


FIG. 1. Derivative of the EPR spectrum from the $[F_{\text{Li}}]^0$ center in CaO:Li as measured at 77 K and 9.5 GHz with the applied magnetic field parallel to the $[100]$ crystal axis. Indicated are the positions of two sets of four lines arising from those centers with the electron-lithium axis parallel to the applied field and those centers with that axis perpendicular to the field. Also indicated is the position of the line arising from isolated F^+ centers.

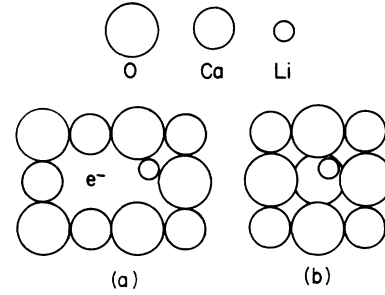


FIG. 2. A schematic diagram of the structure of the $[F_{\text{Li}}]^0$ center in CaO:Li. View (a) is along a perpendicular to the color center lithium axis, while view (b) is along that axis, looking toward the lithium site from the oxygen vacancy. The lithium, which has replaced a calcium, is shown in a postulated off-center position.

SLR measurements on the $[F_{\text{Li}}]^0$ center were made using the pulse saturation and recovery technique. Details of this technique and of the experimental apparatus have been described previously.²¹ The return to thermal equilibrium was not strictly exponential, however, consistent results could be obtained by fitting the recovery signal in the region between 40% and 90% of its thermal equilibrium value.

When $\vec{H}_0 \parallel [100]$, only the $m = -\frac{3}{2}$ hyperfine line is well separated from the remainder of the spectrum. At this orientation, measurements were made only on this line to avoid cross relaxation. The SLR rates between 1.5 and 25 K at two microwave frequencies, 9.51 and 16.49 GHz, are shown in Fig. 3. The rate is a linear function of temperature and is independent of frequency.

The different orientations of the $[F_{\text{Li}}]^0$ center within the crystal are all equivalent with $\vec{H}_0 \parallel [111]$, and only one set of four hf lines is observed. Each line is well resolved, except for the $m = +\frac{1}{2}$ line which partially overlaps the line from the F^+ center. The SLR rates of the remaining three lines as functions of temperature between 5 and 25 K at 9.5 GHz are shown in Fig. 4. Unlike the data for the $[100]$ magnetic-field orientation, these rates increase faster than T at the lowest temperatures, eventually following a linear temperature dependence at higher temperatures. The relaxation rates of the $m = +\frac{3}{2}$ and $m = -\frac{3}{2}$ lines are equal, within experimental error, while the rate of the $m = -\frac{1}{2}$ line is significantly faster.

With the use of fast passage techniques^{22,23} a measurement was made of the SLR rate of the F^+ center in undoped CaO. At 4.2 K and 16 GHz, the rate was approximately $0.03(3) \text{ s}^{-1}$.

The results for the $[F_{\text{Li}}]^0$ center in CaO:Li are

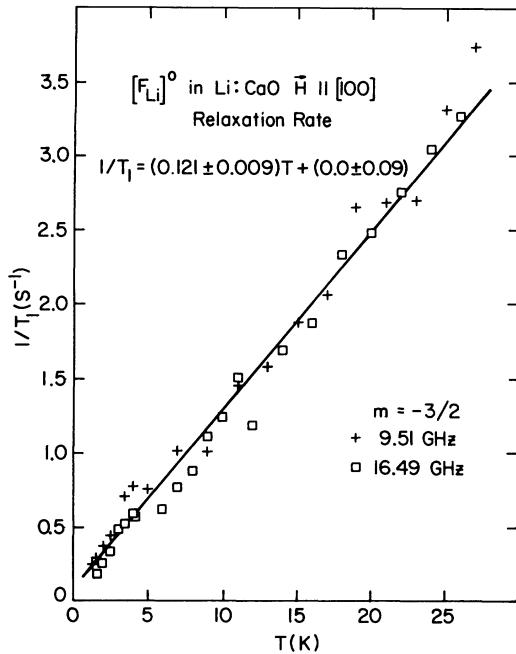


FIG. 3. Spin-lattice relaxation rate of the $[F_{Li}]^0$ center in CaO:Li as measured at microwave frequencies of 9.51 and 16.49 GHz, with the applied magnetic field parallel to the $[100]$ crystal axis. Measurements are on the $m = -\frac{3}{2}$ transition only. The solid curve is the result of the theory described in the text.

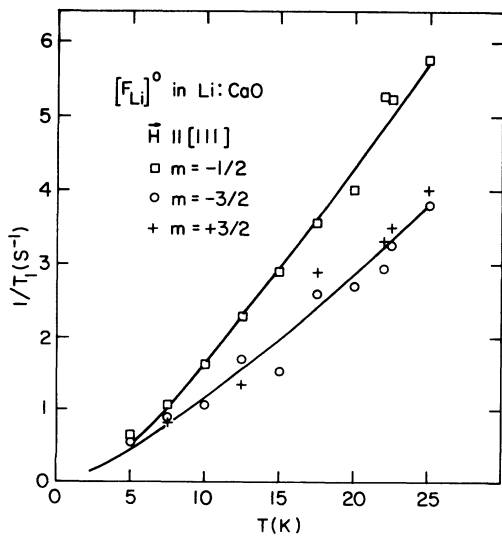


FIG. 4. Spin-lattice relaxation rates of the $[F_{Li}]^0$ center in CaO:Li measured at 9.5 GHz with the applied magnetic field parallel to the crystal $[111]$ axis. Results are shown for three different hyperfine lines. The solid lines are the result of the theory described in the text.

unusual. The rates are fast compared to other F -type centers. At 4.2 K the rate is roughly 30 times that measured in the undoped sample. In the alkali halides rates down to 10^{-3} s^{-1} have been measured.²⁴⁻²⁷ If the relaxation were due to phonon-induced transitions the rate would have a linear dependence on temperature below about 5 K, but a T^7 dependence at higher temperatures.^{25,28-29} Clearly the data cannot be fit to a function of this form. These standard theories of spin-lattice relaxation also predict that the rate will depend on frequency as ν^2 . In the $[100]$ direction there is no discernible frequency dependence. While an anisotropic relaxation rate is neither unusual nor unexpected, what we observe in this system is a change in the functional form of the temperature dependence as the direction of the magnetic field is changed.

III. THEORETICAL INTERPRETATION

The dependence of these data on the nuclear quantum number m indicates that hf interactions play an important role in the relaxation mechanism. For S -state paramagnetic centers such as the $[F_{Li}]^0$, the hf interaction is usually the dominant interaction connecting the electron spin to the lattice phonons. In this material the only nuclear magnetic moment present in significant concentration is the Li dopant (92.6% ^7Li relative abundance, $I = \frac{3}{2}$). Each trapped electron in an $[F_{Li}]^0$ center is adjacent to one of these nuclei. The ionic radius of the Li is significantly smaller than the radius of the calcium it replaces (0.068 nm vs 0.099 nm). In this situation it has often been found that the equilibrium position of the impurity is not the lattice site, but rather that the ion sits "off center."^{1,2} One possible site is shown in Fig. 2. Under these circumstances there will be several local potential minima within which the ion could reside. Quantum-mechanical tunneling between these sites is possible. This generates a splitting of the Li ground-state energy level and produces localized tunneling states (LTS). Phonon-induced transitions between Li tunneling states cause a time variation in the hf interaction which can lead to an electron spin flip. The energy is transferred from the spin system to the LTS system, which we assume is thermalized rapidly. Formally, this is similar to nuclear magnetic resonance in the presence of paramagnetic impurities.³⁰ The $[F_{Li}]^0$ center electron is cast in the role of the nucleus, and the tunneling system plays the role of the paramagnetic impurity.

Following Ref. 14, we can calculate the relaxation of the $[F_{Li}]^0$ center using Fermi's golden rule. The initial and final states are denoted

$$|i\rangle = |M, m, \psi_+, \dots, n_\alpha, \dots\rangle, \quad (2)$$

$$|f\rangle = |M', m', \psi_-, \dots, n_\alpha + 1, \dots\rangle,$$

where $|M\rangle$, $|m\rangle$, $|\psi_+\rangle$, $|\psi_-\rangle$, and $|n_\alpha\rangle$ denote

electron spin, nuclear spin, upper and lower LTS, and phonon states, respectively. The LTS-electron spin interaction Hamiltonian is denoted \mathcal{H}_{TS} and the LTS-phonon Hamiltonian is denoted \mathcal{H}_{TP} . The transition probability is

$$W_{if} = \frac{2\pi}{\hbar} \sum_{\alpha} \left| \frac{\langle M', m', \psi_- | \mathcal{H}_{TS} | M, m, \psi_+ \rangle \langle \psi_+, n_\alpha + 1 | \mathcal{H}_{TP} | \psi_+, n_\alpha \rangle}{-\hbar\omega_\alpha} + \frac{\langle M', m', \psi_- | \mathcal{H}_{TS} | M, m, \psi_- \rangle \langle \psi_-, n_\alpha + 1 | \mathcal{H}_{TP} | \psi_+, n_\alpha \rangle}{-\hbar\omega_\alpha + E} + \frac{\langle \psi_-, n_\alpha + 1 | \mathcal{H}_{TP} | \psi_+, n_\alpha \rangle \langle M', m', \psi_+ | \mathcal{H}_{TS} | M, m, \psi_+ \rangle}{\delta} + \frac{\langle \psi_-, n_\alpha + 1 | \mathcal{H}_{TP} | \psi_-, n_\alpha \rangle \langle M', m', \psi_- | \mathcal{H}_{TS} | M, m, \psi_+ \rangle}{E + \delta} \right|^2 \times (1 + e^{E/kT})^{-1} \delta_D(\hbar\omega_\alpha - E - \delta). \quad (3)$$

In this expression δ is the electron Zeeman energy splitting, δ_D is the energy-conserving Dirac δ function, E is the LTS splitting, and ω_α is the frequency of a phonon of index α . The term $(1 + e^{E/kT})^{-1}$ is the probability of finding the LTS in the ψ_+ state initially. The hyperfine energy splittings have been neglected relative to E and δ .

\mathcal{H}_{TP} has been obtained previously.^{3,4} The LTS Hamiltonian, in the basis corresponding to the ion being localized in one well or the other,³¹ is given by

$$\mathcal{H}'_{LTS} = \frac{1}{2} \begin{pmatrix} \xi & \Delta \\ \Delta & -\xi \end{pmatrix}. \quad (4)$$

Here ξ is the asymmetry of the potential wells and Δ is the overlap energy, given by $\hbar\omega_0 e^{-\lambda}$. The ground state of an isolated well is $\hbar\omega_0$, and $\lambda = (2mV)^{1/2}d/\hbar$, where V is the barrier height, d is the well separation, and m is the mass of the tunneling ion. To obtain the tunneling-state-phonon-interaction Hamiltonian, \mathcal{H}_{TP} , Eq. (4) is expanded in terms of the strain e , and the result is transformed to a basis which diagonalizes \mathcal{H}'_{LTS} . The result is

$$\mathcal{H}_{TP} = \frac{1}{2E} \begin{pmatrix} \xi \frac{\partial \xi}{\partial e} + \Delta \frac{\partial \Delta}{\partial e} & \xi \frac{\partial \Delta}{\partial e} - \Delta \frac{\partial \xi}{\partial e} \\ \xi \frac{\partial \Delta}{\partial e} - \Delta \frac{\partial \xi}{\partial e} & -\xi \frac{\partial \xi}{\partial e} - \Delta \frac{\partial \Delta}{\partial e} \end{pmatrix} \cdot e, \quad (5)$$

where $E = (\xi^2 + \Delta^2)^{1/2}$ is the energy splitting between the two levels. The strain e is then expanded

in phonon operators in the usual way.³²

The tunneling-state-spin interaction can be written

$$\mathcal{H}'_{TS} = \vec{S} \cdot \sum_i \frac{\partial \vec{A}}{\partial x_i} \cdot \vec{I} dx_i, \quad (6)$$

where \vec{A} is the hf tensor and the x_i are direction coordinates. In the earlier work^{13,14} \vec{A} was assumed isotropic, and to fall off with distance R as $1/R^3$. Under these conditions

$$\mathcal{H}'_{TS} = a \vec{I} \cdot \vec{S} \frac{3d}{2R_0} \begin{pmatrix} -1 & 0 \\ 0 & 1 \end{pmatrix} \quad (7a)$$

in the nondiagonal tunneling-state basis, or

$$\mathcal{H}_{TS} = a \vec{I} \cdot \vec{S} \frac{3d}{2R_0 E} \begin{pmatrix} -\xi & \Delta \\ \Delta & \xi \end{pmatrix} \quad (7b)$$

in the diagonal basis. Here R_0 is the average distance of the tunneling ion from the F^+ center, and the tunneling distance d is assumed to be along the color center Li axis.

There are three problems with this Hamiltonian. First, the $[F_{Li}]^0$ center exhibits an anisotropic hf spectrum and SLR rate, neither of which can be predicted using an isotropic hf coupling tensor. Second, in CaO one would expect some, if not most, of the tunneling to be transverse to the color center Li axis. Finally, since the $\vec{I} \cdot \vec{S}$ operator in Eq. (7) cannot connect spin states of the form $|M, m\rangle$ with $|M+1, m\rangle$, this Hamiltonian is inadequate for use in Eq. (3) to restore thermal equilibrium after sa-

turation of an allowed ESR transition.

These defects can be remedied if the anisotropic terms of the hf tensor are included. If the tunneling distance d is small compared to the color center Li distance R_0 , transverse tunneling can be approximated as a rotation of the hf tensor coordinate system. Since the hf interaction is not isotropic this will cause the coupling energy between the electron and the Li to change, inducing spin transitions.

The principal coordinate system for \vec{g} and \vec{A} has the z axis along the color center Li axis. The hf tensor is written

$$\vec{A} = a\vec{1} - b \begin{pmatrix} 1 & 0 & 0 \\ 0 & 1 & 0 \\ 0 & 0 & -2 \end{pmatrix}, \quad (8)$$

where $\vec{1}$ is the identity matrix. Since \vec{g} is approximately isotropic, \vec{S} is quantized along \vec{H}_0 and the hf tensor must be written in a new coordinate system with $\hat{z}' \parallel \vec{H}_0$. The orientation of \hat{z}' will be specified relative to the principal axis system by ρ , the angle between \hat{z}' and the yz plane, and ϕ , the angle between the projection of \hat{z}' onto the yz plane and the \hat{z} axis.

The interaction energy depends only on θ , the angle between \hat{z}' and \hat{z} . When \vec{H}_0 is at an angle θ from \hat{z} , the hf tensor has the form

$$\vec{A}'_0 = a\vec{1} - b \begin{pmatrix} 1 & 0 & 0 \\ 0 & \cos^2\theta - 2\sin^2\theta & 0.5\sin^2\theta \\ 0 & 0.5\sin^2\theta & \sin^2\theta - 2\cos^2\theta \end{pmatrix}. \quad (9)$$

To obtain \mathcal{H}_{TS} we substitute Eq. (9) into Eq. (6), expressing the derivative with respect to x and y as derivatives with respect to θ . If it is assumed that the tunneling in the x, y and $z = r$ directions are independent, this leads to a Hamiltonian with three parts, each of the form

$$\mathcal{H}'_{TS, x_i} = C'_{x_i}(\rho, \phi) T_{x_i}(\theta), \quad (10)$$

where

$$C'_x(\rho, \phi) = \frac{bd}{2R_0} \begin{pmatrix} -1 & 0 \\ 0 & 1 \end{pmatrix} \frac{\sin\rho}{1 - \cos^2\rho \cos^2\phi}, \quad (11a)$$

$$C'_y(\rho, \phi) = \frac{bd}{2R_0} \begin{pmatrix} -1 & 0 \\ 0 & 1 \end{pmatrix} \frac{\cos\rho \sin\phi}{1 - \cos^2\rho \cos^2\phi}, \quad (11b)$$

$$C'_r(\rho, \phi) = \frac{3d}{2R_0} \begin{pmatrix} -1 & 0 \\ 0 & 1 \end{pmatrix}. \quad (11c)$$

Here, as in Eq. (7a), the matrix indicates the tunneling ion is localized in one well or the other.

For $x_i = x$ or y

$$T_{x_i}(\theta) = \frac{1}{4}[1 - 3\sin(2\theta)](I_+S_+ + I_-S_-) + \frac{1}{4}[1 + 3\sin(2\theta)](I_+S_- + I_-S_+) - \frac{3}{2}i \cos(2\theta)(I_zS_+ - I_zS_-) - \frac{3}{2}i \cos(2\theta)(S_zI_+ - S_zI_-) \quad (12)$$

and for $x_i = r$

$$T_r(\theta) = \frac{1}{4}[2a + b(\sin^2\theta - 2\cos^2\theta)](I_+S_- - I_-S_+) + \frac{3}{4}b \sin^2\theta(I_+S_+ - I_-S_-) - \frac{1}{4}ib \sin(2\theta)(I_+S_z - I_-S_z + I_zS_+ - I_zS_-). \quad (13)$$

To complete the calculations, \mathcal{H}'_{TS, x_i} must be transformed to a basis in which \mathcal{H}_{LTS} is diagonal. The effect on the LTS matrices of Eq. (11) can be seen by comparing Eq. (7b) with Eq. (7a). Transition rates can now be calculated by substituting \mathcal{H}_{TS} and \mathcal{H}_{TP} into Eq. (3).

These rates describe a complex relaxation process in which all "adjacent" (e.g., $\Delta M = 0, \pm 1, \Delta m = 0, \pm 1$) nuclear and electron spin states are coupled.

Such a system will not relax to thermal equilibrium with a single time constant, a fact observed experimentally in this study. However, to understand the range of frequency and temperature dependencies which can be predicted by this model it is useful to examine the SLR rate of two isolated states. In this case the recovery is exponential with a time constant

$$\frac{1}{T_1} = W_{if} + W_{fi} + W_{i'f'} + W_{f'i'}, \quad (14)$$

where the primed states differ only in that the initial LTS state is ψ_- .

Case I: $E \gg \delta$. Here the LTS energy E is much greater than the electron Zeeman energy δ and the relaxation rate is given by

$$\frac{1}{T_1} = \frac{3C(\rho, \phi)}{4\pi\rho^*\hbar^4 v^5} |\langle M'm' | T(\theta) | Mm \rangle|^2 \times \frac{1}{E} \left[\frac{G_+}{E^2} + \frac{G_-}{\delta^2} \right] \text{csch} \left[\frac{E}{kT} \right], \quad (15a)$$

where

$$G_+ = \Delta^2 (\xi \partial \xi / \partial e + \Delta \partial \Delta / \partial e)^2, \quad (15b)$$

$$G_- = \xi^2 (\xi \partial \Delta / \partial e - \Delta \partial \xi / \partial e)^2, \quad (15c)$$

ρ^* is the mass density, and v is the velocity of sound of the crystal. The tunneling parameters, E , Δ , ξ , $C(\rho, \phi)$, and $T(\theta)$ vary with tunneling direction and hence have implicit subscripts x_i . For temperatures $T \ll E/k$, $1/T_1$ is a constant. As T increases $1/T_1$ increases faster than T , becoming linear with T at high temperatures. In the limited region corresponding to these measurements ($T < 30$ K) this function appears linear, but with an apparent negative y intercept, whenever $T > (E/2k)$.

The frequency dependence of $1/T_1$ depends on the relative strength of the two LTS-strain coupling terms, G_+ and G_- . Unless $\xi(\partial \Delta / \partial e) \sim \Delta(\partial \xi / \partial e)$, the G_- term of Eq. (15) must dominate due to the relative magnitudes of the energy denominators. In this case the SLR rate will depend on microwave frequency ν as $1/\nu^2$. If the first term should dominate, the rate will be independent of frequency.

Case II: $E \ll \delta$. In the other limit where $E \ll \delta$ the rate is

$$\frac{1}{T_1} = \frac{3C(\rho, \phi)}{4\pi\rho^*\hbar^4 v^5} |\langle M'm' | T(\theta) | Mm \rangle|^2 \times \frac{\delta}{E^4} (G_+ + G_-) \coth \left[\frac{\delta}{2kT} \right]. \quad (16)$$

For experiments performed at X and Ku band, the Zeeman splitting is $\delta = 0.46$ and 0.79 K, respectively, so the condition $\delta \ll kT$ is always satisfied and $\coth(\delta/2kT)$ can be approximated as $2kT/\delta$. The SLR rate is linear in temperature and independent of frequency.

The hf splittings have been neglected in these derivations. This approximation is not valid for $\Delta M = 0$, $\Delta m = \pm 1$ transitions. For those purely nuclear transitions Eqs. (14) and (15) are valid, provided δ is reinterpreted as the hf splitting.

In CaO:Li the transitions are not between two levels, but rather between eight levels as shown by the arrows in Fig. 5. When \vec{H}_0 is oriented along the

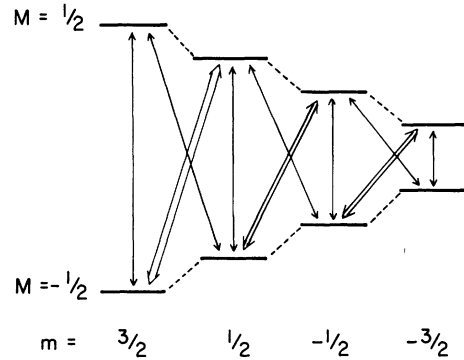


FIG. 5. The energy levels of the coupled electron-spin-nuclear-spin system. The isotropic term in the hyperfine interaction can cause the transitions indicated by the double arrows only. The dashed lines indicate pure nuclear transitions.

[100] direction Eq. (13) predicts that radial tunneling will contribute only to the transitions indicated by double arrows in Fig. 5. Transverse tunneling contributes to all transitions. Radial tunneling may dominate the SLR when $\vec{H}_0 || [111]$, while transverse tunneling dominates when $\vec{H}_0 || [100]$. If for radial tunneling $E \gg \delta$, and for transverse tunneling $E \ll \delta$, then by Eqs. (14) and (15) the SLR rate would be linear for $\vec{H}_0 || [100]$ and be approximately $\text{csch}(E/kT)$ for $\vec{H}_0 || [111]$.

The population of the i th level N_i is governed by the following set of coupled differential equations

$$dN_i/dt = \sum_{j \neq i} [N_j (W_{ji} + W_{j'i'} + R_{ji}) - N_i (W_{ij} + W_{i'j'} + R_{ij})]. \quad (17)$$

In these equations W_{ji} and $W_{j'i'}$ are the transition rates from states j to i and from j' to i' as calculated using Eq. (3). Again the primes indicate that the LTS are initially in the ψ_- state. The R_{ij} represent microwave-induced transition rates. In matrix form, the solution to these equations is

$$\vec{N} = \vec{V} \cdot \vec{E} + \vec{B}, \quad (18)$$

where $E_i = a_i \exp(r_i t)$ and \vec{V} and \vec{B} are constants. The prefactors a_i are determined from the initial conditions; \vec{V} , \vec{B} , and r_i are determined numerically from Eq. (17) using well-known matrix techniques.

For each allowed line in the EPR spectrum the population difference between the two levels involved was calculated as a function of time after the saturating pulse. The maximum time used was such that the population difference was equal to the "noise," as estimated from the experimental signal-

to-noise ratio. These simulated recoveries consisted of a fast, brief, initial recovery, followed by an extended slow recovery. This mimicked the experimental data. These calculated recoveries were fit to a single exponential over the region between 40% and 90% of full recovery, as were the experimental data. The theoretical time constants determined in this manner, scaled to pass through the experimental data at 25 K, appear in Fig. 4.

The temperature dependence of the simulated recoveries was insensitive to the relative values of G_+ and G_- . The two parameters were set equal to G_t for transverse tunneling and to G_r for radial tunneling. In order for radial tunneling to dominate for a [111] magnetic-field orientation, G_r/G_t must exceed 10^6 . If the tunneling-state parameters ξ and Δ were each proportional to the LTS energy E , then $G \propto E^4$ and the reasonable condition that $E_r/E_t > 32$ then suffices.

The exact value of E_t cannot be determined from the data, however, the linear relationship between relaxation rates and temperature, illustrated by Fig. 3, demands that $E_t/k < 0.5$ K. We estimated it to be 0.1 K for our model calculations. From the curvature of the data in Fig. 4, E_r/k was estimated to be 25 K. A reasonable fit to the temperature dependence can be obtained with values of E_r/k between 20 and 35 K. Subject to the constraint that the simulated and experimental relaxation rates agree at a temperature of 25 K, the curves in Fig. 4 can be generated with $E_r/k = 25$ K, $E_t/k = 0.1$ K, $G_r = 10^6 G_t$, and $\vec{H}_0 || [111]$. It is noteworthy that the $m = -\frac{1}{2}$ hf line experimentally relaxes 1.5 times faster than the $m = \pm \frac{3}{2}$ hf lines at 25 K, whereas the simulation predicted a ratio of 0.93. Furthermore, this weak and qualitatively incorrect hf dependence appears in our simulations only when the purely nuclear spin transitions (indicated by the dotted lines in Fig. 5) are excluded from the simulation. Because of these obvious shortcomings in the model with respect to the hf dependence of the SLR rates, we did not attempt to measure the frequency dependence of the hf dependence.

For an external magnetic field along the [100] direction, the simulations correctly predict the linear

temperature dependence of the SLR rates which appear in Fig. 3.

IV. CONCLUSIONS

The dependence of the electron spin-lattice relaxation rate of the $[F_{Li}]^0$ center in CaO:Li on temperature, microwave frequency, and crystal orientation can be explained by assuming that the electron spin relaxes through localized tunneling states created by an "off-center" lithium impurity. The coupling between the electron and the lithium is the hyperfine interaction. The anisotropic nature of this interaction, coupled with the existence of two tunneling motions, one along the electron-nuclear axis, and the other perpendicular to that axis, is crucial to understanding the observed rates.

The radial tunneling energy is roughly 25 K. The lack of frequency dependence when $\vec{H}_0 || [100]$ can be explained in two ways. Either the transverse tunneling energy is less than the Zeeman energy, or the coupling parameter G_+ is much greater than G_- . In the latter case the SLR rate is independent of frequency regardless of tunneling-state energy. However, even in this case the linearity of the SLR rate with temperature for a [100] magnetic-field direction restricts the transverse tunneling energy to be less than 1 K.

Although the existence of an m dependence supports the importance of the hyperfine interaction to the relaxation mechanism, this theory was unable to correctly predict that dependence.

ACKNOWLEDGMENTS

The authors are indebted to M. M. Abraham of the Oak Ridge National Laboratory for providing the samples used in this study, and for providing the results of the EPR and ENDOR (electron-nuclear double resonance) studies of CaO:Li. This paper is based upon a dissertation submitted by D. G. Stinson in partial fulfillment of the requirements for the Ph.D. degree at the University of Illinois. This work was supported by the U.S. Department of Energy, Division of Materials Sciences, under Contract No. DE-AC02-76ER01198.

*Present address: Physics Division Research Laboratories, Eastman Kodak Company, Rochester, New York 14650.

¹V. Narayanamurti and R. O. Pohl, *Rev. Mod. Phys.* **42**, 210 (1970).

²M. V. Klein, in *Physics of Color Centers*, edited by W.

Beall Fowler (Academic, New York, 1968).

³P. W. Anderson, B. I. Halpern, and C. M. Varma, *Philos. Mag.* **25**, 1 (1972).

⁴W. A. Phillips, *J. Low Temp. Phys.* **7**, 351 (1972).

⁵D. W. Feldman, J. G. Castle, Jr., and G. R. Wagner, *Phys. Rev.* **145**, 237 (1966).

- ⁶J. Murphy, *Phys. Rev.* **145**, 241 (1966).
- ⁷H. Ohkura, Y. Mori, and M. Hisshii, *J. Phys. Soc. Jpn.* **31**, 947 (1971).
- ⁸M. F. Deigen, B. D. Shanina, V. S. Vikhnin, I. M. Zaritskii, A. A. Konchits, G. Korradi, R. Vaska, V. M. Maevskii, and V. V. Udod, *Fiz. Tverd. Tela (Leningrad)* **15**, 434 (1973) [*Sov. Phys.—Solid State* **15**, 310 (1973)].
- ⁹H. Ohkura, Y. Mori, M. Matsuoka, T. Watanabe, and A. Satoh, *Prog. Theor. Phys. Suppl.* **57**, 68 (1975).
- ¹⁰H. Ohkura, M. Matsuoka, and Y. Mori, *J. Phys. Soc. Jpn.* **39**, 547 (1975).
- ¹¹H. Ohkura, T. Watanabe, D. Nakamura, and Y. Mori, *J. Phys. Soc. Jpn.* **41**, 707 (1976).
- ¹²Y. Morri and H. Ohkura, *J. Phys. Soc. Jpn.* **50**, 1616 (1981).
- ¹³S. R. Kurtz and H. J. Stapleton, *Phys. Rev. Lett.* **42**, 1773 (1979).
- ¹⁴S. R. Kurtz and H. J. Stapleton, *Phys. Rev. B* **22**, 2195 (1980).
- ¹⁵P. J. Anthony and A. C. Anderson, *Phys. Rev. B* **16**, 3827 (1977).
- ¹⁶P. J. Anthony and A. C. Anderson, *Phys. Rev. B* **14**, 5198 (1976).
- ¹⁷P. J. Anthony and A. C. Anderson, *Phys. Rev. B* **19**, 5310 (1979).
- ¹⁸U. Strom, M. von Schickfus, and S. Hunklinger, *Phys. Rev. Lett.* **41**, 910 (1978).
- ¹⁹M. M. Abraham, C. T. Butler, and Y. Chen, *J. Chem. Phys.* **55**, 3752 (1971).
- ²⁰M. M. Abraham, Y. Chen, D. N. Olson, V. M. Orera, T. M. Wilson, and R. F. Wood, *Phys. Rev. B* **23**, 51 (1981).
- ²¹R. C. Herrick and H. J. Stapleton, *J. Chem. Phys.* **65**, 4778 (1976).
- ²²A. Abraham, *The Principles of Nuclear Magnetism* (Clarendon, Oxford, 1961), p. 65.
- ²³M. Weger, *Bell. Sys. Tech. J.* **39**, 1013 (1960).
- ²⁴H. Seidel and H. C. Wolf, in *Physics of Color Centers*, edited by W. Beall Fowler (Academic, New York, 1968), p. 557.
- ²⁵D. W. Feldman, R. W. Warren, and J. G. Castle, Jr., *Phys. Rev.* **135**, A470 (1964).
- ²⁶R. W. Warren, D. W. Feldman, and J. G. Castle, Jr., *Phys. Rev.* **136**, A1347 (1964).
- ²⁷H. Panepucci and L. F. Mollenauer, *Phys. Rev.* **178**, 589 (1969).
- ²⁸M. F. Deigen and V. Ya. Zevin, *Zh. Eksp. Teor. Fiz.* **39**, 1126 (1960) [*Sov. Phys.—JETP* **12**, 785 (1961)].
- ²⁹V. Ya. Zevin, *Fiz. Tverd. Tela (Leningrad)* **3**, 599 (1961) [*Sov. Phys.—Solid State* **3**, 439 (1961)].
- ³⁰T. J. Schmugge and C. D. Jeffries, *Phys. Rev.* **138**, A1785 (1965).
- ³¹S. Hunklinger and W. A. Arnold, in *Physical Acoustics*, edited by W. P. Mason and R. N. Thurston (Academic, New York, 1976), Vol. 12, p. 155.
- ³²R. Orbach and M. Tachiki, *Phys. Rev.* **127**, 1587 (1962).